scientific reports

Check for updates

OPEN

# In vitro evaluation of the anthelmintic activity of citrus flavonoids against free-living and parasitic nematodes

Krittika Srisuksai[1,2], Nussaba Niyom[1], Poom Adisakwattana[3], Naphatsamon Uthailak[4], Kamonpan Fongsodsri[4], Tapanee Kanjanapruthipong[5], Sumate Ampawong[5], Tipparat Thiangtrongjit[1], Phornpimon Tipthara[6], Joel Tarning[6,7] & Onrapak Reamtong[1]✉

**Helminth infections remain a significant global health and economic burden, and the growing emergence of resistance to frontline anthelmintic drugs such as albendazole and ivermectin underscores the urgent need for novel therapeutic strategies. Flavonoids, a diverse group of plant-derived polyphenolic compounds, have gained attention for their broad-spectrum biological activities, including potential antiparasitic properties. This study aimed to investigate the anthelmintic potential of orange-derived flavonoids using two complementary models: the free-living nematode *Caenorhabditis elegans* (wild-type, albendazole-resistant, and ivermectin-resistant strains) and the muscle-stage larvae of *Trichinella spiralis* as a representative parasitic nematode. Among the five flavonoids tested, quercetin exhibited the strongest anthelmintic activity across all *C. elegans* strains and against *T. spiralis*, while demonstrating minimal cytotoxicity in human cell lines, indicating a favorable safety profile. To investigate its potential mode of action, electron microscopy was employed to assess morphological changes, while a mass spectrometry-based metabolomics approach was used to examine molecular mechanisms in *T. spiralis* treated with quercetin. The results showed that quercetin did not induce detectable morphological alterations but significantly disrupted multiple key metabolic pathways, particularly those associated with energy production, lipid metabolism, and mitochondrial function, indicating a systemic metabolic disturbance. These findings offer new insights into the metabolic effects of orange-derived flavonoids and underscore quercetin as a promising lead candidate for anthelmintic development.**

**Keywords** Nematode, *Trichinella spiralis*, Orange flavonoids, *Caenorhabditis elegans*, Metabolomics

Parasitic nematodes pose significant global health, agricultural, and economic challenges, affecting both humans and animals. In humans, gastrointestinal nematodes such as *Ascaris lumbricoides*, hookworms (*Necator americanus* and *Ancylostoma duodenale*), and *Trichuris trichiura* infect billions worldwide, leading to anemia, malnutrition, growth retardation, and impaired cognitive development, particularly in children from low-resource settings[1]. Other nematodes, including *Trichinella spiralis*, cause trichinellosis through the consumption of undercooked meat, leading to symptoms ranging from gastrointestinal distress to muscle inflammation and, in severe cases, cardiac or neurological complications[2]. The global annual incidence of trichinellosis is estimated to be approximately 10,000 cases, with a mortality rate of about 0.2%. However, serological evidence suggests that up to 11 million individuals may be infected worldwide. Cases of trichinellosis have been documented in 55 countries, representing roughly 27.8% of all nations globally[3]. In 2014, the Food and Agriculture Organization of the United Nations (FAO) and the World Health Organization (WHO) listed *T. spiralis* among the top 10

[1]Department of Molecular Tropical Medicine and Genetics, Faculty of Tropical Medicine, Mahidol University, Bangkok, Thailand. [2]Program in Animal Science, Faculty of Animal Sciences and Agriculture Technology, Silpakorn University, Phetchaburi, Thailand. [3]Department of Helminthology, Faculty of Tropical Medicine, Mahidol University, Bangkok, Thailand. [4]Department of Social and Environmental Medicine, Faculty of Tropical Medicine, Mahidol University, Bangkok, Thailand. [5]Department of Tropical Pathology, Faculty of Tropical Medicine, Mahidol University, Bangkok, Thailand. [6]Mahidol Oxford Tropical Medicine Research Unit, Faculty of Tropical Medicine, Mahidol University, Bangkok, Thailand. [7]Centre for Tropical Medicine and Global Health, Nuffield Department of Clinical Medicine, University of Oxford, Oxford, UK. ✉email: onrapak.rea@mahidol.ac.th

most common foodborne parasites that eventually lead to serious health problems[4]. *T. spiralis* is transmitted through the consumption of raw or undercooked meat containing encysted larvae, primarily from pigs or wild animals. The parasite maintains both domestic and sylvatic cycles—pigs acquire infection by ingesting infected tissues, while wild carnivores and scavengers sustain transmission through predation and cannibalism. Humans are accidental hosts, acquiring infection via contaminated meat, thus representing a dead-end in the parasite's life cycle.

In animals, parasitic nematodes significantly reduce livestock productivity by decreasing weight gain, milk production, and reproductive performance, resulting in considerable economic losses for farmers globally[5]. Moreover, several nematodes are zoonotic, such as *T. spiralis* and *Toxocara spp.*, increasing the risk of transmission between animals and humans and highlighting the urgent need for integrated "One Health" approaches. Albendazole (ABZ) and ivermectin (IVM) are widely regarded as the gold standard for treating nematode infections due to their broad-spectrum activity and clinical efficacy[6]. ABZ, a benzimidazole derivative, functions by selectively binding to β-tubulin, thereby preventing its dimerization with α-tubulin and inhibiting microtubule formation within nematode cells, ultimately disrupting essential cellular processes[7]. In contrast, IVM, a macrocyclic lactone, targets the α-subunit of glutamate-gated chloride channel receptors in nematode nerve and muscle cells. This binding enhances chloride ion influx, causing hyperpolarization, leading to paralysis, impaired feeding, reduced fecundity, and eventual death of motile stages[8]. Despite their effectiveness, reliance on ABZ and IVM poses serious challenges. Widespread and repeated usage has led to the emergence of anthelmintic resistance across multiple nematode species, compromising drug efficacy and threatening sustainable control efforts[9]. This growing resistance, combined with persistent environmental contamination, limited access to clean water, and poor sanitation, underscores an urgent need for novel therapeutic strategies. To address these challenges, comprehensive approaches are required, including improved diagnostic tools, integrated control programs, and the development of new anthelmintic agents with distinct modes of action. Advancing drug discovery pipelines will be critical to mitigating the global health and economic burdens posed by parasitic nematodes.

Flavonoids are naturally occurring plant-derived compounds that exhibit a broad spectrum of biological activities, including antioxidant, anti-inflammatory, antimicrobial, and antiparasitic effects[10–12]. Citrus fruits, particularly oranges, are a rich source of flavonoids, predominantly concentrated in the peels, pulp, and seeds. Orange flavonoids are mainly classified into three principal types: flavanones, flavones, and flavonols[13]. Several studies have identified key flavonoids in oranges, such as apigenin, hesperetin, naringin, quercetin, and tangeretin[11,14]. Apigenin, a compound found in traditional medicines, is recognized as a bioactive flavonoid with antioxidant, anti-inflammatory, antihypertensive, antimicrobial, and antiparasitic activities[15,16]. Apigenin has antiprotozoal activity in vitro against *Leishmania amazonensis* and in vivo against visceral leishmaniasis by oral administration[17,18]. Hesperetin is a bioactive flavonoid whose bioactivities include antioxidant, anti-inflammatory, antivirus, and antiparasitic effects[19–21]. Naringin is a natural flavonoid that is abundant in vegetables and fruits. Studies revealed that naringin possesses multiple pharmacological activities, including antioxidant, anti-inflammatory, anti-apoptosis, and anti-diabetes[22,23]. Naringin demonstrated a potent anti-plasmodial effect against *Plasmodium falciparum* through its anti-inflammatory properties[24]. Quercetin is widely used in traditional medicine due to its therapeutic potential, such as antioxidant, anti-inflammatory, antiviral, anticancer, antimicrobial, antiprotozoal, and anthelmintic activities[25–28]. Ethnopharmacological studies on tangeretin have revealed several properties, including antioxidant, anti-inflammatory, and anticarcinogenic[29,30]. Throughout the prolonged history of consuming these flavonoid compounds as part of the daily diet, no harmful effects have been seen[30,31]. The pharmacological potential of these polyphenolic compounds explained why they are among the most popular plant-derived flavonoids. Accumulating evidence highlights the potential of flavonoids as natural anthelmintic agents. Experimental in vitro and in vivo studies have demonstrated their efficacy against a range of helminths, including *Haemonchus contortus*, *Schistosoma mansoni*, *Trypanosoma brucei brucei*, *and Toxocara canis*[32–35]. Notably, kaempferol treatment in *Trichinella spiralis*-infected mice significantly reduced parasite burden and ameliorated intestinal inflammation[36]. Despite these promising findings, few studies have focused on the use of orange-derived flavonoids as potential anthelmintic agents, and the mechanisms by which they exert their effects against parasitic nematodes remain poorly understood. This knowledge gap highlights the need for further investigation, which this study aims to address.

Metabolomics integrates biological experimentation with high-throughput analytical technologies, particularly mass spectrometry, alongside bioinformatics for comprehensive metabolite profiling[37]. By quantitatively and qualitatively characterizing metabolites—the intermediates and end products of cellular metabolism—metabolomics can distinguish between normal and pathological pathways, thereby aiding in disease diagnosis and prognosis prediction[38]. Recent studies have successfully applied metabolomic profiling in parasitology to unravel host-parasite interactions and identify potential therapeutic targets in several helminths, including *Onchocerca volvulus*, *Schistosoma japonicum*, *Toxocara canis*, and *T. spiralis*[39–42]. Leveraging metabolomics in the study of flavonoid activity against parasitic nematodes could therefore provide new insights into their mechanisms of action and metabolic vulnerabilities, facilitating the discovery of novel antiparasitic drug candidates.

In this study, we evaluated the anthelmintic potential of orange-derived flavonoids using *Caenorhabditis elegans* as a nematode model, including wild-type, albendazole (ABZ)-resistant, and ivermectin (IVM)-resistant strains. Additionally, their efficacy was assessed against *T. spiralis* larvae to establish activity in a parasitic nematode model. The cytotoxicity of orange flavonoids was also tested on human cell lines to evaluate safety. To investigate their systemic effects on *T. spiralis*, a mass spectrometry-based metabolomics approach was employed. The half-maximal effective concentration ($EC_{50}$) of the flavonoids was determined, and ultrastructural changes induced by flavonoid treatment were visualized using transmission electron microscopy (TEM). Furthermore,

differential metabolite profiling and pathway analysis were conducted to elucidate the molecular mechanisms underlying the anthelmintic effects of orange flavonoids.

## Materials and methods

### Anthelmintic activity of orange flavonoids on C. elegans

Wild-type N2, albendazole-resistant CB347, and ivermectin-resistant JD608 strains of *Caenorhabditis elegans*, obtained from the Caenorhabditis Genetics Center (CGC, University of Minnesota, USA), were maintained on nematode growth medium (NGM) plates seeded with *Escherichia coli* OP50[43]. The NGM was prepared according to the standard protocol from the *Caenorhabditis Genetics Center* (CGC, University of Minnesota, USA) using reagents purchased from Sigma-Aldrich (St. Louis, US): 3 g NaCl (S9888), 2.5 g peptone (P5905), and 17 g agar (A5306) per liter of distilled water, supplemented with 1 mL of 1 M $MgSO_4$ (M7506), 1 mL of 1 M $CaCl_2$ (C4901), 25 mL of 1 M $KPO_4$ buffer, pH 6.0 (prepared from $KH_2PO_4$, P5655, and $K_2HPO_4$, P3786), and 1 mL of 5 mg/mL cholesterol solution (C8667) added after autoclaving. For synchronization, worms were collected in M9 buffer (3 g $KH_2PO_4$, 6 g $Na_2HPO_4$, 5 g NaCl, 1 mL 1 M $MgSO_4$, distilled water) and subjected to bleaching. Eggs were transferred to unseeded NGM plates and incubated at 20 °C until the L1 stage (~24 h).

For drug testing, apigenin (Cat. No. 10798), hesperetin (H4125), naringin (91842), quercetin (PHR1488), and tangeretin (91004) (Sigma-Aldrich, Switzerland) were dissolved in M9 buffer to achieve final concentrations of 10, 100, 1,000, 10,000, and 100,000 ng/mL, with 0.5% DMSO included in each well. This concentration range facilitates the identification of the therapeutic window and is consistent with established practices in pharmacological research[44].

Negative controls contained 0.5% DMSO, while albendazole and ivermectin were used as positive controls. Thirty L1 worms were dispensed into each well (triplicate) and incubated for 72 h at 20 °C. Worm motility was assessed under an inverted microscope by observing the movement of the worms after compound exposure. The degree of motility was scored visually on a qualitative scale, where a complete lack of movement was defined as death, and any visible movement was considered alive[45]. $EC_{50}$ values were determined by nonlinear regression, and statistical comparisons were performed using one-way ANOVA followed by Dunnett's post-hoc test, with statistical significance set at $P < 0.05$ (GraphPad Prism 9). All experiments were performed in three independent replicates[46].

### Cytotoxicity testing

HepG2 and Caco-2 cell lines were employed to evaluate the cytotoxic effects of orange-derived flavonoids. Cells were seeded in 96-well plates (20,000 cells/well) and maintained in Eagle's minimum essential medium (MEM) supplemented with 10% fetal bovine serum (HyClone, GE Healthcare Life Science, USA) at 37 °C in a humidified atmosphere with 5% $CO_2$ for 24 h. The culture medium was subsequently replaced with the test compounds—apigenin, hesperetin, naringin, quercetin, tangeretin, albendazole (ABZ), and ivermectin (IVM)—at final concentrations of 10, 100, 1,000, 10,000, and 100,000 ng/mL, prepared in MEM with 0.5% DMSO per well. Negative controls contained 0.5% DMSO, while albendazole and ivermectin were used as positive controls. After a further 24 h of incubation, 10 µL of MTT solution (5 mg/mL; AppliChem GmbH, Germany) was added to each well, followed by 4 h incubation under the same culture conditions. The medium was subsequently replaced with a solubilization buffer (4 mM HCl and 0.1% Nonidet P-40 in isopropanol) to dissolve the formazan crystals. Absorbance was recorded at 590 nm with a reference at 620 nm. Cell viability was expressed relative to untreated controls, and the 50% cytotoxic concentration ($CC_{50}$) was determined using nonlinear regression. Statistical comparisons were performed using one-way ANOVA followed by Dunnett's post-hoc test, with statistical significance set at $P < 0.05$ in GraphPad Prism version 9. All assays were conducted in three independent replicates[46].

### Anthelmintic activity of apigenin and quercetin on *T. spiralis* muscle stage

The mice used in this study were purchased from Mahidol University National Laboratory Animal Center, Thailand. The *T. spiralis* strain used in this study was a clinical isolate that has been maintained long-term in the Animal Care Unit, Faculty of Tropical Medicine, Mahidol University. Eight-week-old female ICR mice were orally inoculated with 100 *T. spiralis* larvae. After 60 days of infection, the animals were euthanized by $CO_2$ exposure, and muscle-stage larvae (L1) were recovered from skeletal tissue by enzymatic digestion with 0.7% pepsin and 0.7% HCl. The isolated larvae were maintained in RPMI medium supplemented with 10% fetal calf serum, 200 U/mL penicillin, and 200 µg/mL streptomycin.

For $EC_{50}$ determination, apigenin and quercetin were prepared in RPMI medium (supplemented as described above) at final concentrations of 10, 100, 1,000, 10,000, and 100,000 ng/mL, with 0.5% DMSO included in each well. Negative controls contained 0.5% DMSO, while albendazole (ABZ) and ivermectin (IVM) were included as positive controls. Thirty larvae were transferred into each well in triplicate and incubated for 72 h at 37 °C. Larval motility was scored under an inverted microscope, with live larvae exhibiting free movement, whereas dead larvae showed a C-shaped or linear body and showed no movement. $EC_{50}$ values were calculated using nonlinear regression. Statistical comparisons were performed using one-way ANOVA followed by Dunnett's post-hoc test, with statistical significance set at $P < 0.05$ in GraphPad Prism version 9. All experiments were performed in three independent replicates (adapted from[46].

### Preparation of specimen for transmission electron microscopy

*T. spiralis*-treated were initially treated with quercetin at the $EC_{50}$ value, and sequentially fixed with 2.5% glutaraldehyde and 1% osmium tetroxide (1 h each). The fixed samples underwent dehydration through a graded ethanol series, infiltrated with increasing concentrations of LR white resin (EMS®, USA), embedded in

pure LR white resin, and then polymerized at 60 °C for 48 h. After polymerization, thin sections were cut into 100 nm sections using an ultramicrotome for subsequent immunogold labeling.

### Immunogold labeling technique

To investigate the effects of quercetin treatment and explore the correlation between metabolomic and morphological alterations in *T. spiralis*, immunoelectron microscopy was performed as described in our previous studies[47] using specific antibodies. The primary antibodies targeted markers of mitochondrial function, including translocase of outer mitochondrial membrane 20 (TOM20), a mitochondrial outer membrane receptor that plays a crucial role in mitochondrial biogenesis[48], and succinate dehydrogenase subunit D (SDHD), a subunit of mitochondrial complex II that associates with muscular dysfunction[49], along with Bcl-2 associated X (BAX), a pro-apoptotic protein initiating apoptosis[50]. Briefly, the thin sections were blocked for non-specific binding with 50 mM glycine in phosphate-buffered saline (PBS) and incubated in 5% bovine serum albumin (BSA; EMS®, USA) in PBS. Primary antibodies targeting mitochondrial function, including anti-succinate dehydrogenase (SDHD; MyBioSource, USA, MBS7000340), anti-TOM20 (MyBioSource, USA, MBS2400038), and anti-BAX (MyBioSource, USA, MBS9600035), were diluted 1:50 and added to the sections for 1 h. After incubation, GAR IgG conjugated with 25 nm gold particles (EMS®, USA) was applied for 1 h. To enhance the visibility of the gold particles, a silver enhancement was used for 30 min using the Aurion R-Gent SE-EM kit (EMS®, USA). The sections were then counterstained with uranyl acetate and lead citrate. Ultrastructural features and the distribution of immunogold labeling in *T. spiralis* were examined under TEM (HT7700 model, Hitachi, Japan).

### Metabolomics analysis of quercetin-treated *T. spiralis* muscle larvae

*T. spiralis* larvae treated with 0.5% DMSO served as controls, while larvae exposed to the $EC_{50}$ concentration of quercetin were processed for metabolite extraction as described by[41]. Samples were homogenized in 500 µL of cold methanol, snap-frozen in liquid nitrogen, thawed, and centrifuged at 800 ×g for 1 min at 4 °C. The supernatant was collected, and the extraction was repeated. Supernatants from both extractions were combined. The remaining pellet was resuspended in 250 µL of deionized water, frozen in liquid nitrogen, thawed, and centrifuged at 15,000 ×g for 1 min at 4 °C. This supernatant was pooled with the previous extracts. The combined extracts were centrifuged again at 15,000 ×g for 1 min at 4 °C to remove residual debris, and the clarified supernatant was collected and dried using a speed vacuum concentrator. Three biological replicates and two technical replicates were performed for metabolomics analysis.

### Identification of metabolome using mass spectrometry

Metabolomic analysis was conducted following an established protocol[51]. Briefly, chromatographic separation was achieved using a high-performance liquid chromatography system (Agilent 1260 Quaternary Pump, Agilent 1260 Autosampler, and Agilent 1290 Thermostatted Column Compartment SL; Agilent Technologies, CA, USA) coupled to a quadrupole time-of-flight mass spectrometer (TripleTOF 5600+, SCIEX, USA) equipped with a DuoSpray electrospray ionization (ESI) source. Mobile phase A consisted of 0.1% formic acid in water, while mobile phase B contained 0.1% formic acid in acetonitrile.

Dried metabolite extracts were dissolved in 200 µL of a 1:1 (v/v) mixture of mobile phases A and B, and 100 µL was transferred to LC vials and maintained at 6 °C in the autosampler. A 5 µL aliquot was injected onto a reversed-phase C18 column (ACQUITY UPLC BEH, 2.1 × 100 mm, 1.7 µm; Waters, USA) operated at 40 °C with a flow rate of 0.3 mL/min. The gradient program was as follows: 5% B for 0–2.0 min, 5–60% B from 2.0 to 2.5 min, 60–80% B from 2.5 to 4.0 min, 80–100% B from 4.0 to 12.0 min, held at 100% B until 17.0 min, decreased to 5% B at 17.1 min, and re-equilibrated at 5% B until 20.0 min.

Mass spectrometric detection was carried out in both positive and negative ESI modes using Analyst Software v1.7 (SCIEX). Data were acquired in information-dependent acquisition (IDA) mode, consisting of a TOF-MS survey scan (m/z 100–1000) followed by ten dependent product ion scans (m/z 50–1000) in high-sensitivity mode with dynamic background subtraction. To ensure reproducibility and system stability, pooled quality control (QC) samples were injected at the beginning, intermittently throughout, and at the end of the analytical sequence.

### Data processing and statistical analysis

Metabolomic mass spectra files obtained from LC–MS/MS (.wiff and .wiff.scan) in both + ESI and -ESI modes were separately processed using MS-DIAL software[52]. Alignment parameters were set to a retention time tolerance of 0.1 min and a mass accuracy of 0.015 Da. The compound detection, alignment, and identification were performed using two databases: ESI(+)-MS/MS from authentic standards and ESI(-)-MS/MS from authentic standards. The peak tables containing accurate *m/z* values, retention times, and peak intensities were exported and subsequently analyzed using MetaboAnalyst 6.0 (https://www.metaboanalyst.ca/) under the *Statistical Analysis (one factor)* module. Data were filtered using the interquartile range (IQR), normalized by quantile normalization, transformed by cube root transformation, and scaled by data range scaling. For visualization, Principal Component Analysis (PCA), Partial Least Squares–Discriminant Analysis (PLS-DA), volcano plot, and pathway analysis were generated. PCA and PLS-DA were displayed with 95% confidence intervals, while volcano plots were constructed using $\log_2$ fold-change and –log p-values. Differential metabolites were identified based on a cut-off of fold change > 1.5 and $p < 0.01$. Pathway analysis was conducted using MetaboAnalyst, and pathways with $p < 0.01$ were considered statistically significant. Annotation of putative metabolites was performed using MS-DIAL software.

| Flavonoid | $EC_{50}$ (μM) | | |
|---|---|---|---|
| | N2 | CB347 | JD608 |
| Apigenin | 218.50 ± 11.16 | 55.82 ± 4.89 | 51.33 ± 1.46 |
| Hesperetin | 282.97 ± 23.87 | > 1,000 | 51.71 ± 2.92 |
| Naringin | > 1,000 | > 1,000 | > 1,000 |
| Quercetin | 80.45 ± 20.34 | 76.25 ± 7.40 | 45.28 ± 4.92 |
| Tangeretin | > 1,000 | > 1,000 | 43.11 ± 11.25 |
| ABZ | 672.17 ± 72.97 | > 1,000 | 788.35 ± 22.64 |
| IVM | 17.67 ± 1.85 | 15.40 ± 6.07 | 642.03 ± 56.66 |

**Table 1**. In vitro anthelmintic activity on *C. elegans* (N2, CB347, JD608 strain) of orange flavonoids. $EC_{50}$ is the concentration of flavonoid associated with 50% of the maximum effect against the strain of *C. elegans* evaluated. Results are reported as mean ± S.E.

| Flavonoid | $CC_{50}$ (μM) | |
|---|---|---|
| | HepG2 | Caco-2 |
| Apigenin | 53.31 ± 4.52 | > 1,000 |
| Hesperetin | > 1,000 | 56.30 ± 6.18 |
| Naringin | > 1,000 | 249.03 ± 65.30 |
| Quercetin | > 1,000 | > 1,000 |
| Tangeretin | 251.30 ± 34.96 | 531.27 ± 70.31 |
| ABZ | > 1000 | > 1000 |
| IVM | 14.92 ± 1.39 | 19.98 ± 5.28 |

**Table 2**. Cytotoxicity of orange flavonoids against HepG2 and Caco-2 cells. $CC_{50}$ is the flavonoid concentration associated with 50% of maximum cytotoxic effect against the HepG2 and Caco-2 cell lines. Results are reported as mean ± S.E.

## Results

### In vitro nematocidal activities of orange flavonoids against *C. elegans*

In vitro assays were conducted to evaluate the anti-nematode activity of orange flavonoids against *C. elegans*, including the wild-type N2 strain, the albendazole-resistant CB347 strain, and the ivermectin-resistant JD608 strain. For the *C. elegans* N2 strain, $EC_{50}$ values for apigenin, hesperetin, naringin, quercetin, and tangeretin were 218.50 ± 11.16, 282.97 ± 23.87, > 1,000, 80.45 ± 20.34, and > 1,000 μM, respectively. The positive controls (ABZ and IVM) exhibited $EC_{50}$ values of 672.17 ± 72.97 and 17.67 ± 1.85 μM, respectively (Table 1). Among the tested compounds, the nematocidal activity against the N2 strain was highest for ivermectin (IVM), followed by quercetin, apigenin, hesperetin, albendazole (ABZ), and the lowest activity was observed for naringin and tangeretin.

Against the *C. elegans* CB347 strain, $EC_{50}$ values were 55.82 ± 4.89 μM for apigenin and 76.25 ± 7.40 μM for quercetin, while hesperetin, naringin, and tangeretin all showed $EC_{50}$ values greater than 1,000 μM. The positive controls (ABZ and IVM) exhibited $EC_{50}$ values of > 1,000 and 15.40 ± 6.07 μM, respectively (Table 1). The nematocidal activity against the CB347 strain was in the order: IVM > apigenin > quercetin > hesperetin, naringin, tangeretin, and ABZ.

In the assessment against the *C. elegans* JD608 strain, $EC_{50}$ values for apigenin, hesperetin, naringin, quercetin, and tangeretin were 51.33 ± 1.46, 51.71 ± 2.92, > 1,000, 45.28 ± 4.92, and 43.11 ± 11.25 μM, respectively. The positive controls (ABZ and IVM) exhibited the $EC_{50}$ values of 788.35 ± 22.64 and 642.03 ± 56.66 μM, respectively (Table 1). Among the tested compounds, the nematocidal activity against the JD608 strain was highest for tangeretin, followed by quercetin, apigenin, hesperetin, ivermectin (IVM), albendazole (ABZ), and the lowest activity was observed for naringin.

### In vitro cytotoxicity of orange flavonoids against Caco-2 cells

This assay has been widely used to measure in vitro cytotoxicity effects of compounds and standard drugs in cell lines. The results showed a $CC_{50}$ of apigenin, hesperetin, naringin, quercetin, and tangeretin of 53.31 ± 4.52, > 1,000, > 1,000, > 1,000, and 251.30 ± 34.96 μM on the HepG2 cell line, respectively. The positive controls of ABZ and IVM resulted in a $CC_{50}$ of > 1000 and 14.92 ± 1.39 μM, respectively, on the same cell line (Table 2). In addition, the results showed a $CC_{50}$ of apigenin, hesperetin, naringin, quercetin, and tangeretin of > 1,000, 56.30 ± 6.18, 249.03 ± 65.30, > 1,000, and 531.27 ± 70.31 μM, respectively, on the Caco-2 cell line while the positive control (ABZ and IVM) resulted in a $CC_{50}$ of > 1000 and 19.98 ± 5.28 μM, respectively (Table 2). Based on these findings, apigenin and quercetin exhibited the most potent anti-nematode activity (Table 1), while simultaneously showing the lowest cytotoxicity among all compounds. Therefore, apigenin and quercetin were chosen for subsequent *T. spiralis* testing.

| Flavonoid | $EC_{50}$ (μM) |
|---|---|
| Apigenin | > 1,000 |
| Quercetin | 146.54 ± 28.24 |
| ABZ | 128.67 ± 34.09 |
| IVM | 106.69 ± 7.89 |

**Table 3**. In vitro anthelmintic activity on *T. spiralis* of apigenin and quercetin. The $EC_{50}$ represents the concentration of each flavonoid that produces 50% of the maximum effect against *T. spiralis*. Results are expressed as the mean ± standard error (S.E.). The selectivity index (SI) is defined as the ratio of $CC_{50}$ to $EC_{50}$, while "n/a" indicates data not available.

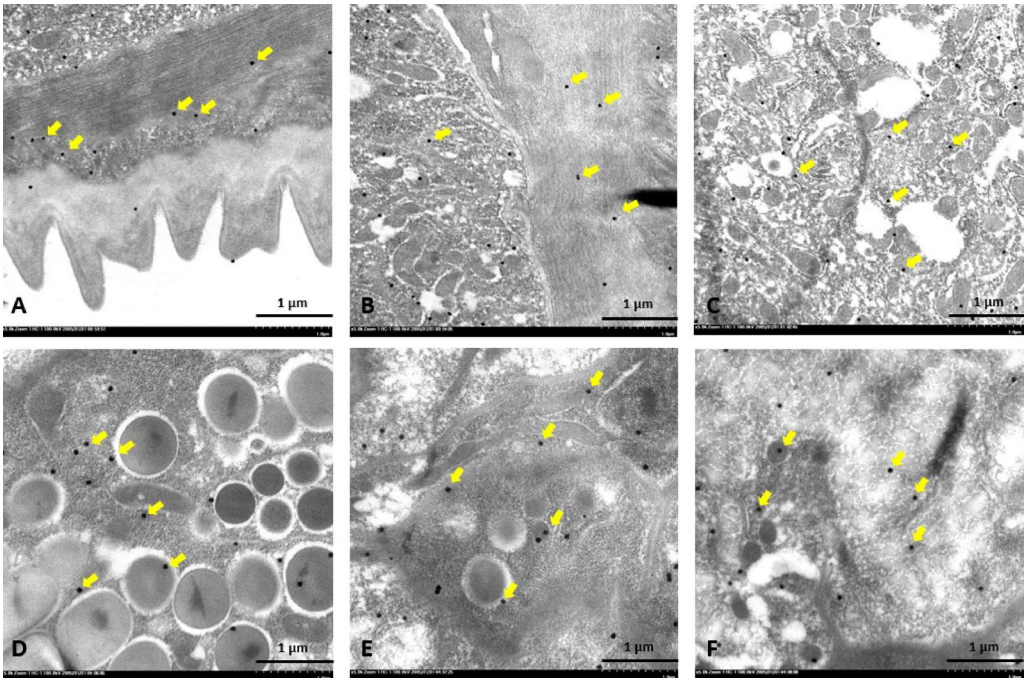


**Fig. 1**. Electron microscopic immunogold labeling of TOM20 in *Trichinella spiralis* from control and quercetin-treated groups. Transmission electron microscopy (TEM) images show the control group (**A**–**C**) and quercetin treatment group (**D**–**F**). Yellow arrows indicate immunolocalization of TOM20 in the *T. spiralis* samples.

## In vitro nematocidal activities of apigenin and quercetin against *T. spiralis*

In vitro testing assessed the anti-nematode activity of apigenin and quercetin against *T. spiralis*. The results showed an $EC_{50}$ of apigenin at > 1,000 μM and quercetin at 146.54 ± 28.24 μM on the *T. spiralis*. In addition, the positive control (ABZ and IVM) showed an $EC_{50}$ of 128.67 ± 34.09 and 106.69 ± 7.89 μM, respectively, on the *T. spiralis* (Table 3). The nematocidal activity of our chosen compounds and positive controls against *T. spiralis* was in the order IVM > ABZ > quercetin and apigenin.

## Effects of quercetin treatment on mitochondrial function, apoptosis, and morphological changes

To assess the effects of quercetin treatment on mitochondrial function, apoptosis, and morphological changes in *T. spiralis*, immunogold TEM was conducted. In summary, no apparent ultrastructural changes were observed in the treatment group across the cuticular layer, muscular area, or coelomic space compared to the non-treatment. Immunoreactivity of TOM20 and SDHD was more prominent than that of BAX, with signals detected throughout all three regions. Quantitative immunolocalization was examined across various regions of the parasite, including the cuticle, muscle, and internal structures. The results showed that the expression levels of TOM20, SDHD, and BAX were comparable between the quercetin-treated and control groups. Interestingly, although muscle tissue is typically prone to structural alterations, the muscle ultrastructure appeared well-preserved in both groups. The qualitative examination of each marker between the treated and control groups was illustrated in Figs. 1 and 2, 3 and 4.

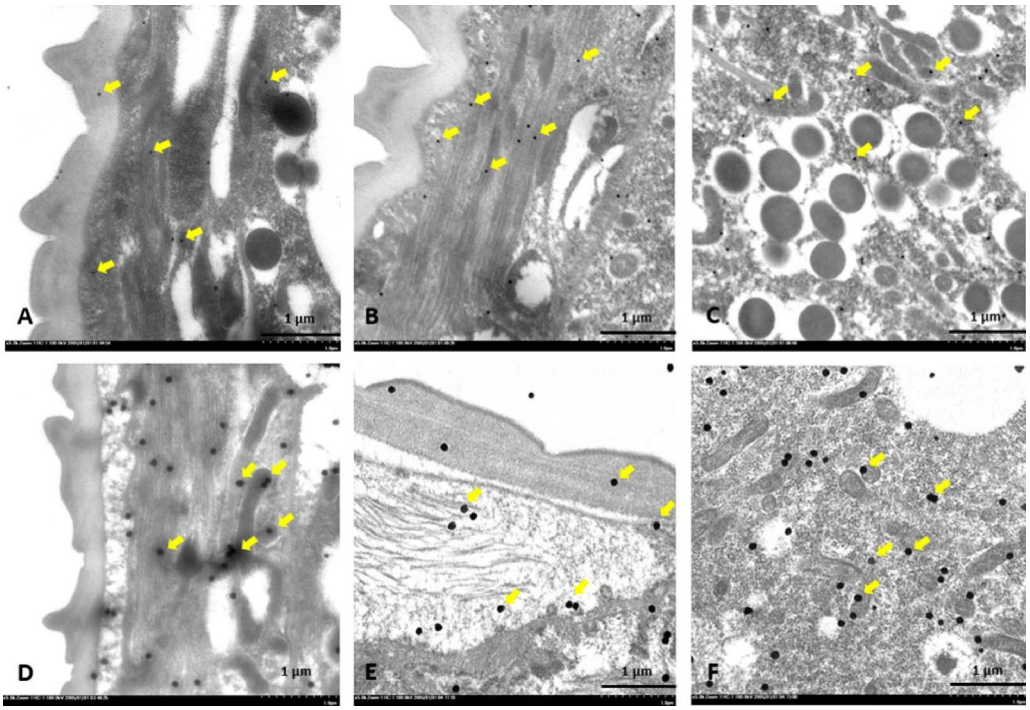


**Fig. 2**. Immunogold localization of SDHD in *T. spiralis* from control and quercetin-treated groups. The images show the control group (**A**–**C**) and quercetin treatment group (**D**–**F**). Yellow arrows indicate the SDHD immunolabelling in the *T. spiralis* samples.

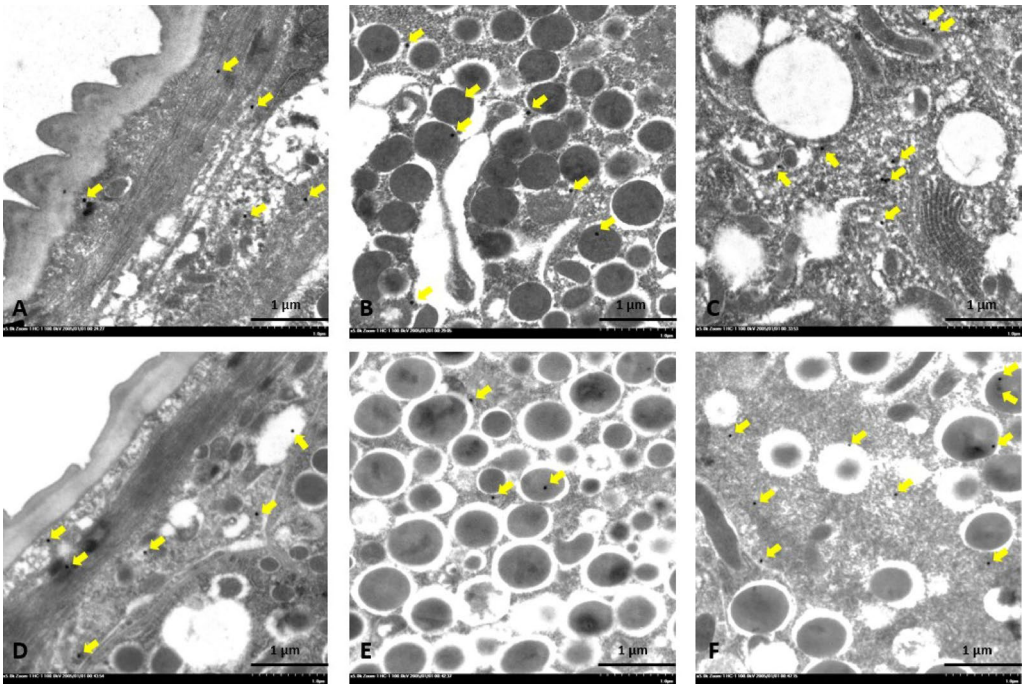


**Fig. 3**. Immunogold labelling of BAX in *T. spiralis* from control and quercetin-treated groups. The TEM images show *T. spiralis* from the control group (**A**–**C**) and the quercetin-treated group (**D**–**F**). BAX protein localization is indicated by yellow arrows.

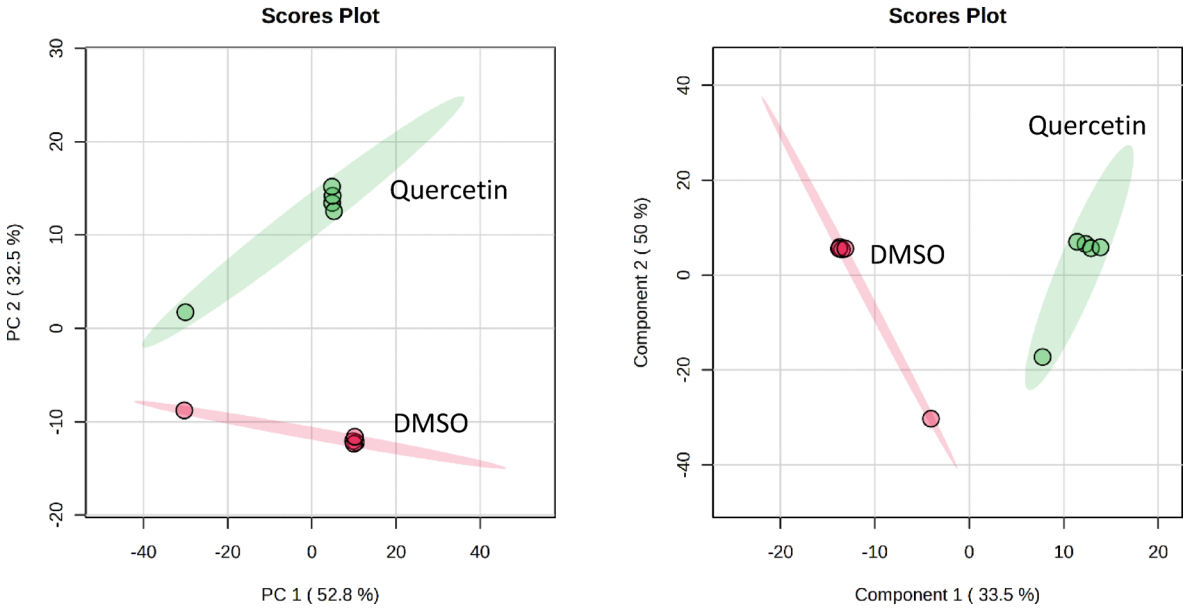


**Fig. 4**. Multivariate analysis of metabolite profiles from *T. spiralis* treated with DMSO (red circles) or quercetin (green circles), using partial least squares-discriminant analysis (PLS-DA).

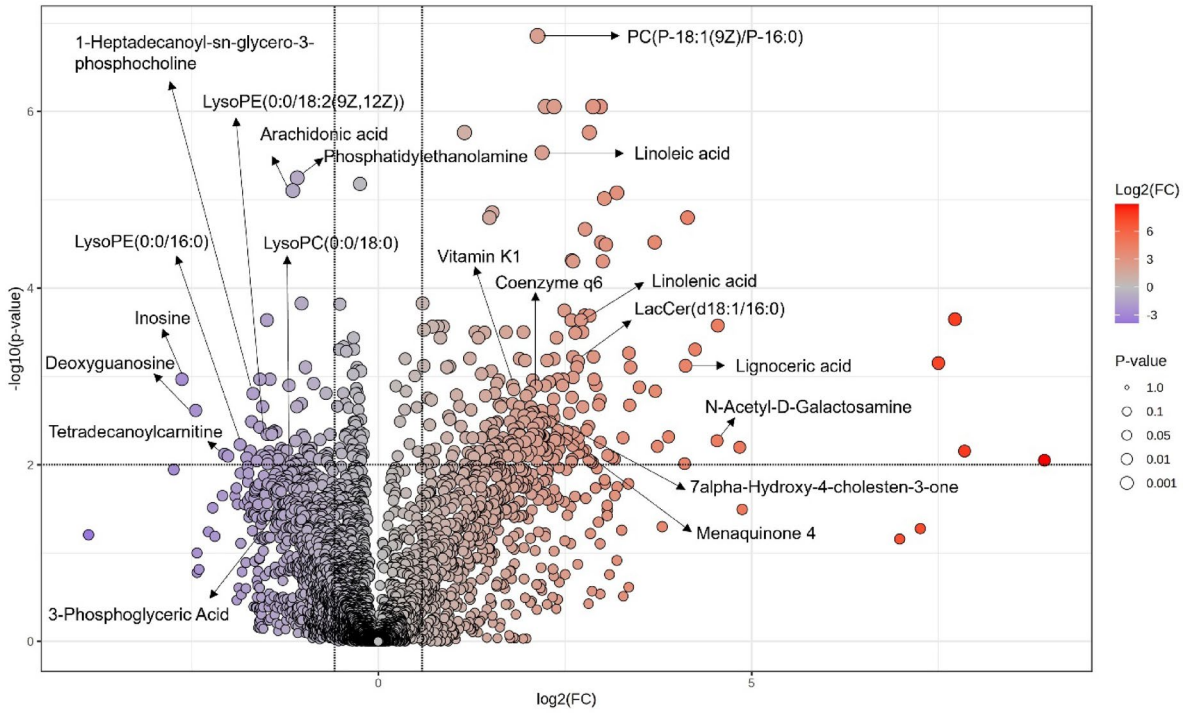


**Fig. 5**. Volcano plot analysis, illustrating up-regulated and down-regulated metabolites after treatment with quercetin. The two vertical lines indicate a ± 1.5-fold change compared to DMSO control. The horizontal line represents a statistically significant difference at a p-value < 0.01. Blue and red circles refer to down- and up-regulated metabolites, respectively.

## Metabolite profiles of *T. spiralis* treated with quercetin

A volcano plot was created to display the statistical significance and the fold change between DMSO control and quercetin treatment (Fig. 5). After exposure to quercetin, 272 differential features showed a p-value < 0.01 and > 1.5-fold change. Around 204 features were up-regulated, and 68 were down-regulated. The most up-regulated metabolites, following treatment with quercetin were N-Acetyl-D-Galactosamine, lignoceric acid, and linolenic

| No. | Potential metabolites | m/z | Mass Error (Da) | Log2 (FC) | *p*-Value |
|---|---|---|---|---|---|
| 1 | N-Acetyl-D-Galactosamine | 222.09782 | 0.00061 | 4.5233 | 0.0070919 |
| 2 | Lignoceric acid | 369.38321 | 0.01050 | 4.0956 | 0.0001014 |
| 3 | Linolenic acid | 277.21588 | 0.00144 | 2.7081 | 0.0004623 |
| 4 | LacCer(d18:1/16:0) | 862.64905 | 0.02405 | 2.6728 | 0.0006945 |
| 5 | Menaquinone 4 | 445.31357 | 0.00345 | 2.2163 | 0.0060384 |
| 6 | Linoleic acid | 279.23306 | 0.00012 | 2.1922 | 0.0000702 |
| 7 | 7alpha-Hydroxy-4-cholesten-3-one | 423.33130 | 0.00794 | 2.1364 | 0.0037187 |
| 8 | PC(P-18:1(9Z)/P-16:0) | 760.57977 | 0.00531 | 2.1307 | 0.0000043 |
| 9 | Coenzyme q6 | 597.45886 | 0.00989 | 1.8385 | 0.0021506 |
| 10 | Vitamin K1 | 473.34482 | 0.00482 | 1.8127 | 0.0017177 |

**Table 4**. Top-ten up-regulated metabolites of *T. spiralis* after treatment with quercetin.

| No. | Potential metabolites | m/z | Mass Error (Da) | Log2 (FC) | *p*-Value |
|---|---|---|---|---|---|
| 1 | Inosine | 291.07080 | 0.00079 | -2.6373 | 0.0008150 |
| 2 | Deoxyguanosine | 290.08514 | 0.00083 | -2.4539 | 0.0024828 |
| 3 | Tetradecanoylcarnitine | 372.30997 | 0.00085 | -2.0664 | 0.0074963 |
| 4 | LysoPE(0:0/16:0) | 452.27704 | 0.00122 | -1.8636 | 0.0077011 |
| 5 | 1-Heptadecanoyl-sn-glycero-3-phosphocholine | 510.35422 | 0.00119 | -1.6835 | 0.0008150 |
| 6 | LysoPE(0:0/18:2(9Z,12Z)) | 476.27423 | 0.00403 | -1.4991 | 0.0018140 |
| 7 | LysoPC(0:0/18:0) | 546.35083 | 0.00220 | -1.4886 | 0.0085352 |
| 8 | Arachidonic acid | 303.23309 | 0.00015 | -1.1472 | 0.0003581 |
| 9 | Phosphatidylethanolamine | 528.30853 | 0.00104 | -1.0876 | 0.0001535 |
| 10 | 3-Phosphoglyceric Acid | 186.99202 | 0.00819 | -1.0514 | 0.0059161 |

**Table 5**. Top-ten down-regulated metabolites of *T. spiralis* after treatment with quercetin.

acid, as measured by the fold change (Table 4). The most down-regulated metabolites after treatment with quercetin were inosine, deoxyguanosine, and tetradecanoylcarnitine (Table 5).

Ranking the top three metabolites based on their impact on metabolic pathways revealed significant enrichment in the following processes: RORA-mediated activation of gene expression, BMAL1:CLOCK/NPAS2-driven circadian gene expression, and SREBF (SREBP)-regulated gene expression (Fig. 6).

## Discussion

Current antinematode drugs, including benzimidazoles, macrocyclic lactones, imidazothiazoles, and tetrahydropyrimidines, are limited in number and have been in use for decades, leading to increasing drug resistance in livestock parasites and emerging reduced efficacy in human nematodes. Many agents show stage-specific activity, with poor effectiveness against larval or encysted stages, and variable cure rates across species, often resulting in treatment failures in mass drug administration programs. Adverse effects, contraindications in pregnancy, and pharmacokinetic limitations such as low solubility, poor absorption, and inadequate tissue penetration further hinder their utility. Moreover, the absence of combination therapies and a weak drug development pipeline, driven by low commercial incentives, restrict innovation and exacerbate the reliance on aging drugs with diminishing effectiveness. In the urgent search for alternative therapeutics against parasitic nematodes, significant attention has turned to plant-derived metabolites, particularly flavonoids, which have demonstrated promising anthelmintic potential[10]. In this study, we evaluated the anthelmintic activity of orange flavonoids using a *C. elegans* model to assess their effects on both drug-sensitive and drug-resistant strains. *C. elegans* is widely recognized as a preferred model for anthelmintic research due to its ease of cultivation under laboratory conditions, well-characterized genetics, and extensive molecular toolkit[53]. In this study, we employed three *C. elegans* strains including N2 (wild type), CB347 (albendazole-resistant), and JD608 (ivermectin-resistant) to evaluate the anthelmintic activity of orange flavonoids. As expected, the positive controls, IVM and ABZ, exhibited $EC_{50}$ values consistent with their respective resistance profiles. Notably, our ABZ findings align with previous reports indicating that *C. elegans* displays limited sensitivity to ABZ[54]. Remarkably, all three strains showed lower $EC_{50}$ values when treated with apigenin and quercetin, with both flavonoids demonstrating greater potency than ABZ (Table 1). Apigenin and quercetin, a member of the flavonoid family, are present in a wide variety of plant-derived foods such as oranges, lemons, berries, onions, apples, or black tea[17,55]. Apigenin has a wide range of reported biological effects including antioxidant, cancer chemopreventive, antihypertensive, anti-inflammatory, antimicrobial and antiprotozoal activities[15,56]. Dietary quercetin consumption has been associated to different health benefits, including anticancer, anti-inflammatory, antioxidant, and neuroprotective activities[55,57,58]. According to previous reports, the crude extract of *Artemisia campestris*, which contains apigenin and quercetin, exhibited anthelminthic activity against both the eggs and adult stages of *Haemonchus*

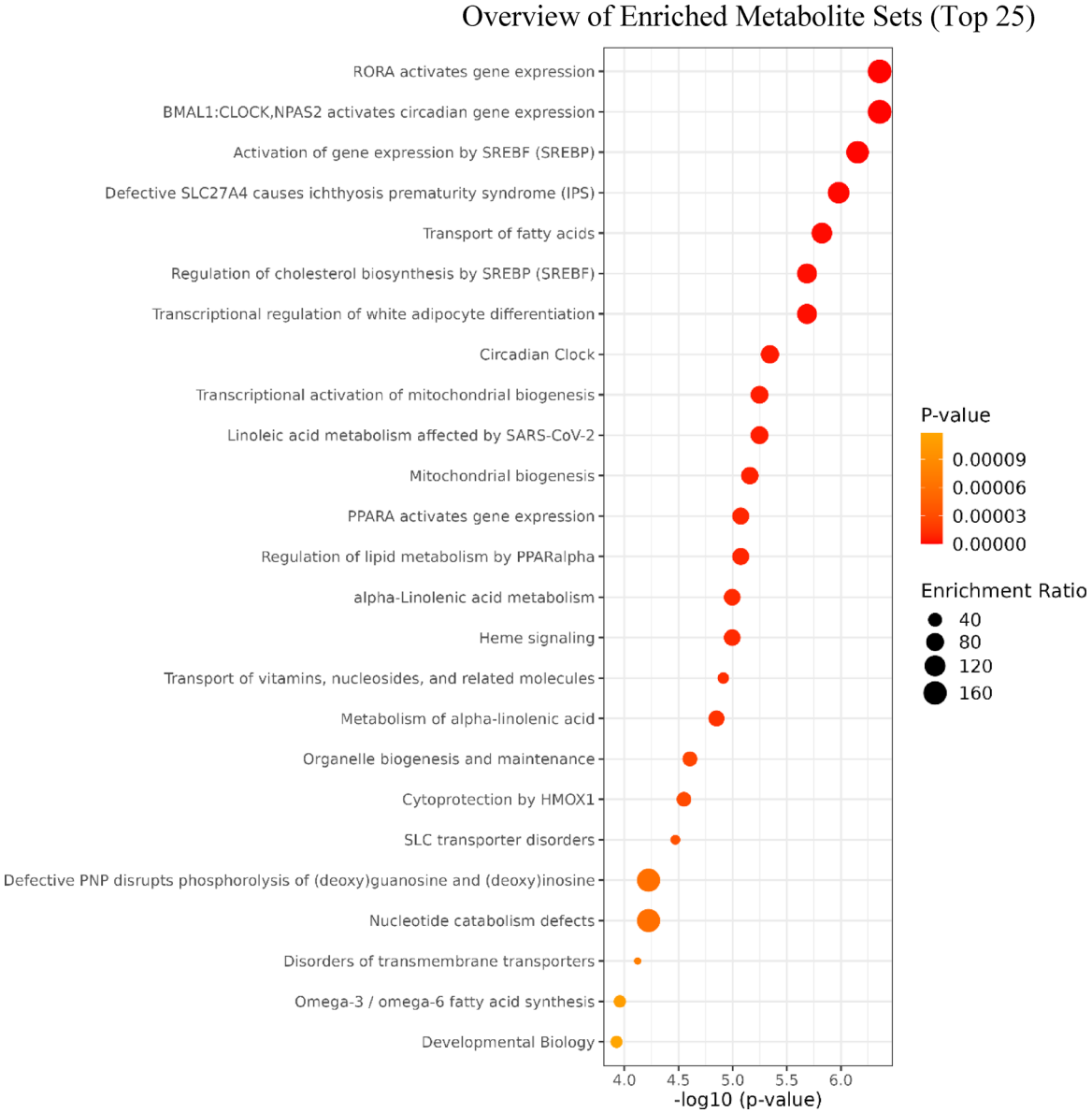


**Fig. 6**. Pathway analysis of the differential *T. spiralis* metabolite between DMSO and quercetin treatment.

*contortus*[59]. In both in vitro and in vivo studies, apigenin significantly enhanced the antimicrobial activity of colistin against multidrug-resistant Enterobacteriaceae, including mcr-1-positive strains[60]. Quercetin has been reported to be effective against both chloroquine-sensitive and chloroquine-resistant *Plasmodium falciparum* by targeting the lactate dehydrogenase active site[61]. In addition, quercetin induced mortality and ultrastructure changes in *T. canis* third-stage larvae compared with the control and ABZ-treated groups[33].

HepG2 is a widely used hepatic cell line which is utilized in various research areas, including liver oncogenesis and the evaluation of substance-induced cytotoxicity[62]. The human Caco-2 cell line is widely used as an in vitro model of the intestinal epithelial barrier that is mainly used for assessing the bioavailability of drugs or test compounds[63]. This study found that the orange flavonoid exhibited $CC_{50}$ values comparable to those of the anthelmintic agents ivermectin (IVM) and albendazole (ABZ) in both HepG2 and Caco-2 cells (Table 2). In clinical trials, ABZ treatment induced hepatitis in infant and adult humans by elevating liver enzymes[64,65]. Case studies report IVM-induced liver injury as hepatitis, hepatocellular injury, cholestasis, increased levels of alanine aminotransferase and aspartate aminotransferase, and abnormal liver function tests[66,67]. Furthermore, there have been reported that IVM-treated rats show thinner circular and longitudinal muscular layers in the small intestine, which can result in slower intestinal transit times[68]. Interestingly, quercetin showed the highest $CC_{50}$ value among the orange flavonoids in both HepG2 and Caco-2 cells (Table 2). This suggests that quercetin is least likely to induce hepatotoxicity or intestinal cytotoxicity compared to apigenin, ABZ, and IVM at the same concentration. Previous studies have demonstrated that quercetin exhibits hepatoprotective activity through several mechanisms such as antioxidant, anti-inflammatory, anti-apoptotic, and lipid metabolism regulation[69,70]. Dietary quercetin enhances the intestinal barrier function through the assembly of tight junction proteins

and the expression of claudin-4, which results from inhibition of a protein kinase C isoform[71]. Furthermore, dietary quercetin could alleviate inflammatory damage, maintain intestinal barrier function, and modulate gut microbiota in lipopolysaccharide-induced laying hens[72]. Similar to our study, mice treated with the high dose of apigenin showed liver damage through oxidative stress[73,74].

In the *T. spiralis* assay, quercetin demonstrated a lower $EC_{50}$ than apigenin and exhibited potency within the same range as ABZ. (Table 2). According to the flavonoid structures (Supplementary Fig. 1), glycosylated flavonoids such as naringin are bulkier and exhibit lower bioavailability due to reduced membrane permeability, while methoxylated derivatives like tangeretin are highly lipophilic and form fewer hydrogen bonds with biological targets. In contrast, quercetin's intermediate polarity facilitates efficient membrane diffusion while retaining sufficient hydrogen-bonding capacity for strong interactions with enzyme active sites and other biomolecular targets. This balanced physicochemical profile likely enhances its absorption, distribution, and binding affinity within nematode systems, thereby contributing to its pronounced anthelmintic efficacy. The molecular effect of quercetin on the *T. spiralis* has not been previously investigated, although the anthelmintic effect of quercetin has been demonstrated in other helminth infections. Quercetin showed cestocidal activity against *Hymenolepis diminuta*, with an $EC_{50}$ of 12.03 mg/mL after 2 h exposure. Electron microscopy revealed extensive damage to the suckers and neck region, as well as deformed, shrunken, wrinkled proglottids in treated worms[27]. Quercetin showed anthelmintic activity against all of the development stages of *Haemonchus contortus* though generation of oxidative stress[10]. Moreover, quercetin against *Toxocara canis*, with exposure at $LC_{90}$ (0.55 mM) causing marked body shrinkage, swelling of the cuticle and caudal papillae, and erosion of cuticular annulations under electron microscope[75]. However, the $EC_{50}$ of quercetin did not cause ultrastructure changes across the cuticular layer, muscular area, or coelomic space in *T. spiralis*. In addition, the expression levels of TOM20, SDHD, and BAX were not significantly different between the quercetin-treated and control groups (Figs. 1, 2 and 3). Consistent with previous study, no ultrastructure changes were observed despite the ability to eliminate the parasites[76].

Metabolomic analysis revealed that the most up-regulated metabolite following quercetin treatment was N-acetyl-D-galactosamine (GalNAc), the initiating sugar in most O-linked glycans present in helminth glycoproteins[77]. O-linked glycans are particularly abundant in the muscle-stage larvae (L1) of *T. spiralis*[78]. Surface carbohydrates in helminths play crucial roles in adhesion to host cells, immune evasion, and host–parasite communication[79,80]. Drug-induced damage to the parasite's surface coat can lead to cleavage of GalNAc-rich glycoproteins and glycolipids, releasing GalNAc into the surrounding environment or cytosol. Therefore, Thus, the observed upregulation of GalNAc likely reflects a quercetin-induced disruption of surface glycan structures, which compromises essential cellular interactions and contributes to nematode death. Lignoceric acid, linolenic acid, and linoleic acid were also up-regulated in *T. spiralis* following quercetin treatment. Helminth fatty acids are vital components of membrane lipid composition[81]. The observed up-regulation likely represents a parasite stress response, as antiparasitic drugs can compromise membrane integrity either directly or indirectly, triggering increased synthesis of structural fatty acids such as the very-long-chain saturated lignoceric acid and polyunsaturated fatty acids like linoleic and linolenic acids to restore or strengthen damaged membranes. However, prolonged metabolic imbalance in lipid remodeling can disrupt membrane homeostasis, ultimately leading to loss of cellular integrity and parasite death. The most down-regulated metabolites following quercetin exposure were inosine and deoxyguanosine. Inosine and other small molecules have been identified in helminth parasites[82]. Inosine, a purine nucleoside, is generated either through adenosine degradation or via 5′-nucleotidase activity on inosine monophosphate (IMP)[83]. IMP is a central precursor for guanosine monophosphate, which is subsequently converted to deoxyguanosine monophosphate, an essential DNA building block[84]. Starvation for even a single DNA precursor can be sufficient to induce cell death[85]. Therefore, the observed depletion of both DNA precursors may contribute to the parasite death, induced by quercetin treatment.

According to pathway analysis, quercetin's effect on the RORA–circadian system pathway may contribute to parasite death by disrupting key regulatory processes that maintain parasite homeostasis. RORA, through its control of circadian rhythm genes such as BMAL1, coordinates metabolism, stress responses, and immune modulation[86,87]. In parasites, circadian regulation influences essential functions including nutrient utilization, replication timing, and adaptation to host immune cycles[88]. Therefore, quercetin-induced alterations in the RORA–circadian signaling pathway could impair metabolic synchronization and weaken the parasite's ability to adapt to host immunity, ultimately leading to cellular dysfunction and death.

Quercetin's impact on the PPARA pathway may contribute to parasite death by disrupting the tight link between energy metabolism and stress adaptation. PPARA is a transcription factor that regulates genes involved in glucose and lipid metabolism as well as inflammation-modulating pathways[89]. In parasites, efficient lipid utilization and metabolic flexibility are essential for growth, reproduction, and adaptation to host environments. By altering PPARA activity, quercetin may impair fatty acid oxidation, disrupt energy balance, and reduce the availability of key lipid-derived structural components for membranes. Additionally, modulation of inflammation-related pathways could shift the host–parasite interaction toward conditions that favor immune clearance. In Leishmania infections, for example, activation of PPARγ by curcumin suppresses IFNγ and nitric oxide production, thereby increasing parasite burden[90]. Together, these metabolic and immune disruptions can compromise parasite survival and lead to death.

Quercetin was found to affect sterol regulatory element-binding proteins (SREBPs). The SREBPs are key transcription factors that control the expression of genes involved in lipid metabolism[91]. Lipids are important components of the cell and organelle membrane of *T. spiralis*. They act as signaling molecules in the intracellular information transmission of parasites[92]. The transport and utilization of fatty acids is critical for their survival and proliferation within the host. A previous study indicated that long-chain fatty acid transport protein 1 (FATP1) plays an essential role in lipid metabolism, moulting, and the development of *T. spiralis*[93]. Another study found that *C. elegans* treated with alpha-linoleic acids showed increased lifespan via activation of the NHR-49/

PPARα and SKN-1/Nrf2 transcription factor[94]. Helminths tend to concentrate linoleic acid series in their tissues relative to host serum, suggesting selective synthesis or accumulation to regulate membrane composition during growth[95]. Lipid metabolism enzymes have been proposed as "chokepoint" for helminth survival and potential targets for anthelmintic drug discovery[96].

Quercetin was found to influence the mitochondrial biogenesis pathway, the process of generating new mitochondria, which is essential for repairing tissue damage and restoring cellular energy by replacing impaired mitochondria[97]. Given that mitochondrial injury can disrupt energy production, activation of this pathway may represent a stress response to quercetin treatment. Notably, depletion of TbTob55, a protein involved in mitochondrial biogenesis, has been shown to cause death of *Trypanosoma brucei* at the procyclic stage[98], suggesting that quercetin's impact on this pathway could contribute to parasite lethality.

Although this study successfully demonstrated the anthelmintic effects of quercetin against *T. spiralis* through the disruption of multiple key metabolic pathways, several limitations should be acknowledged. First, quantitative evaluation of immunogold labeling based on gold particle density measurements was not feasible due to inherent technical variability in sample preparation, section thickness, and antibody accessibility within *T. spiralis* larvae. To ensure interpretative accuracy, the immunogold TEM analysis was therefore performed qualitatively, emphasizing the presence, spatial distribution, and relative density of gold particles rather than absolute quantification. Second, the absence of in vivo validation limits the assessment of the compound's efficacy and safety within a physiological context. Third, pharmacokinetic constraints, including variability in absorption and metabolism, may influence quercetin's bioavailability and therapeutic potential. Notably, quercetin exhibits poor oral bioavailability (<5%), while the observed $EC_{50}$ values (45–146 μM) may exceed achievable plasma concentrations. Fourth, the mechanistic investigations were conducted at a single concentration, which may not fully capture the dose–response relationship under in vivo conditions. Finally, combination therapy was not explored in this study, although it could provide valuable insights into potential synergistic effects. These limitations should be carefully considered and addressed in future research to strengthen the translational relevance of the findings.

In conclusion, this study demonstrates that quercetin have profound anthelmintic effects against *T. spiralis* through multiple pathways, including inflammation, lipid metabolism, and mitochondrial biogenesis. Interestingly, quercetin exhibited no cytotoxicity effects on the human cell. Taken together, quercetin can be a lead molecule for the development of a new drug for the treatment of *T. spiralis* and its associated complications.

## Data availability

All the mass spectrometry data have been deposited in the Science Data Bank repository with accession number 10.57760/sciencedb.27176 (https://www.scidb.cn/en/anonymous/VnJ1WUZi).

Received: 10 September 2025; Accepted: 24 December 2025
Published online: 26 December 2025

## References

1. Stepek, G., Buttle, D. J., Duce, I. R. & Behnke, J. M. Human Gastrointestinal nematode infections: are new control methods required? *Int. J. Exp. Pathol.* **87**(5), 325–341. https://doi.org/10.1111/j.1365-2613.2006.00495.x (2006).
2. Gottstein, B., Pozio, E. & Nöckler, K. Epidemiology, diagnosis, treatment, and control of trichinellosis. *Clin. Microbiol. Rev.* **22**, 127–145 (2009).
3. Taha, N. M., Youssef, F. S., Auda, H. M., El-Bahy, M. M. & Ramadan, R. M. Efficacy of silver nanoparticles against *Trichinella spiralis* in mice and the role of multivitamin in alleviating its toxicity. *Sci. Rep.* **14**, 5843 (2024).
4. El-kady, A. M. et al. A potential herbal therapeutic for trichinellosis. *Front. Vet. Sci.* **9**, 970327 (2022).
5. Kaplan, R. M. Drug resistance in nematodes of veterinary importance: a status report. *Trends Parasitol.* **20**(10), 477–481. https://doi.org/10.1016/j.pt.2004.08.001 (2004).
6. Elmehy, D. A. et al. Niosomal versus nana-crystalline Ivermectin against different stages of *Trichinella spiralis* infection in mice. *Parasitol. Res.* **120**, 2641–2658 (2021).
7. Puspitasari, S., Farajallah, A., Sulistiawati, E. & Muladno Effectiveness of Ivermectin and albendazole against *Haemonchus contortus* in sheep in West Java, Indonesia. *Trop. Life Sci. Res.* **27**(1), 135–144 (2016).
8. Kaji, M. D., Noonan, J. D., Geary, T. G. & Beech, R. N. Structural mechanism underlying the differential effects of Ivermectin and moxidectin on the *C. elegans* glutamate-gated chloride channel GLC-2. *Biomed. Pharmacother.* **145**, 112380 (2022).
9. Doyle, S. R. et al. Genomic landscape of drug response reveals mediators of anthelmintic resistance. *Cell. Rep.* **41**(3), 111522. https://doi.org/10.1016/j.celrep.2022.111522 (2022).
10. Goel, V., Sharma, S., Chakroborty, N. K., Singla, L. D. & Choudhury, D. Targeting the nervous system of the parasitic worm, *Harmonchus contortus* with Quercetin. *Heliyon* **9**, e13699 (2023).
11. Pereira, R. M. S. et al. Quantification of flavonoids in Brazilian orange peels and industrial orange juice processing wastes. *Agric. Sci.* **8**, 631–644 (2017).
12. Silva, L. P., Debiage, R. R., Bronzel-Júnior, J. L. & da Silva, R. M. G. Mello-Peixoto, E. C. T. *In vitro* anthelminthic activity of *Psidium Guajava* hydroalcoholic extract against gastro-intestinal sheep nematodes. *Acad. Bras. Ciênc.* **92**, e20190074 (2020).
13. Addi, M. et al. An overview of bioactive flavonoids from *Citrus* fruits. *Appl. Sci.* **12**, 29 (2022).
14. Liew, S. S., Ho, W. Y., Yeap, S. K. & Sharifudin, S. A. B. Phytochemical composition and *in vitro* antioxidant activities of *Citrus sinensis* Peel extracts. *PeerJ* **6**, e5331 (2018).
15. Fonseca-Silva, F., Inacio, J. D. F., Canto-Cavalheiro, M. M., Menna-Barreto, R. F. S. & Almeida-Amaral, E. E. Oral efficacy of apigenin against cutaneous leishmaniasis: involvement of reactive oxygen species and autophagy as a mechanism of action. *PLoS Negl. Trop. Dis.* **10**(2), e0004442 (2016).
16. Chen, P. et al. Apigenin exhibits anti-inflammatory effects in LPS-stimulated BV2 microglia through activating GSK3β/Nrf2 signaling pathway. *Immunopharmacol. Immunotoxicol.* **42**(1), 9–16 (2020).
17. Emiliano, Y. S. S. Almeida-amaral, E. E. Apigenin is a promising molecule for treatment of visceral leishmaniasis. *Front. Cell. Infect. Microbiol.* **13**, 1066407 (2023).
18. Fonseca-Silva, F., Canto-Cavalheiro, M. M., Menna-Barreto, R. F. S. & Almeida-Amaral, E. E. Effect of apigenin on *Leishmania amazonensis* is associated with reactive oxygen species production followed by mitochondrial dysfunction. *J. Nat. Prod.* **78**(4), 880–884 (2015).

19. Bai, X. et al. The protective effect of the natural compound Hesperetin against fulminant hepatitis *in vivo* and *in vitro*. *Br. J. Pharmacol.* **174**(1), 41–56 (2017).
20. Eberle, R. J. et al. *Vitro* study of Hesperetin and hesperidin as inhibitors of Zika and Chikungunya virus proteases. *PLoS ONE.* **16**(3), e0246319 (2021).
21. I.P. Rocha, S. et al. Antileishmanial activity of Hesperetin on leishmania donovani, in vitro and in Silico Inhibition of acetylcholinesterase and investigation of the targets sterol C-24 reductase and N-myristoyltransferase. *Exp. Parasitol.* **270**, 108903 (2025).
22. Cai, J. et al. Naringenin: a Flavanone with anti-inflammatory and anti-infective properties. *Biomed. Pharmacother.* **164**, 114990 (2023).
23. Shilpa, V. S. et al. Phytochemical properties, extraction, and Pharmacological benefits of natingin: a review. *Molecules* **28**, 5623 (2023).
24. Bhatt, D. et al. Naringin and chloroquine combination mitigates chloroquine-resistant parasite-induced malaria pathogenesis by attenuating the inflammatory response. *Phytomedicine* **133**, 155943 (2024).
25. Aghababaei, F. & Hadidi, M. Recent advances in potential health benefits of Quercetin. *Pharmaceuticals* **16**, 1020 (2023).
26. Lam, H. Y. P., Huang, Y-T., Liang, T-R. & Peng, S-Y. *In vivo* screening of flavonoids compounds revealed Quercetin as a potential drug to improve recovery of angiostrongyliasis after albendazole treatment. *PLoS Negl. Trop. Dis.* **18**(9), e0012526 (2024).
27. Ray, M. S., Mondal, C., Saha, S., Mandal, S. & Lyndem, L. M. Quercetin: an anthelmintic potential against zoonotic tapeworm *Hymenolepis diminuta* (Rudolphi, 1819). *J. Helminthol.* **99**, 1–11 (2025).
28. Xu, D., Hu, M., Wang, Y. & Cui, Y. Antioxidant activities of Quercetin and its complexes for medicinal application. *Molecules* **24**, 1123 (2019).
29. Arafa, E. A., Shurrab, N. T. & Buabeid, M. A. Therapeutic implications of a polymethoxylated flavone, tangeretin, in the management of cancer via modulation of different molecular pathways. *Adv. Pharmacol. Pharm. Sci.* **2021**, 4709818 (2021).
30. Wani, I. et al. An update on the potential of Tangeretin in the management of neuroinflammation-mediated neurodegenerative disorder. *Life* **14**, 504 (2024).
31. Harwood, M. et al. A critical review of the data related to the safety of Quercetin and lack of evidence of in vivo toxicity, including lack of genotoxic/carcinogenic properties. *Food chem. Toxicol.* **45**(11), 2179–2205 (2007).
32. Allam, G. & Abuelsaad, A. S. A. *In vitro* and *in vivo* effects of hesperidin treatment on adult worms of *Schistosoma mansoni*. *J. Helminthol.* **88**, 362–370 (2014).
33. Elmahy, R. A., Moustafa, A. Y. & Radwan, N. A. *Toxocara canis*: prospective activity of Quercetin and venom of *Cassiopea Andromeda* (Cnidaria: Cassiopeidae) against third-stage larvae *in vitro*. *J. Exp. Zool. Ecol. Integr. Physiol.* **341**, 991–1001 (2024).
34. Mohammed, Y. A. et al. Rutin-rich flavonoid subtraction of *Annona senegalensis* mitigates *Trypanosoma brucei brucei* infection and hematobiochemical changes in infected mice. *Biomed Res. Int.* **2023**, 6820338 (2023).
35. Oliveira, A. F. et al. Anthelmintic activity of plant extracts from Brazilian savanna. *Vet. Parasitol.* **236**, 121–127 (2017).
36. Maged, A. I. A., Metwally, K. M., El-Menyawy, H. M., Hegab, F. & El-Wakil, E. Assessment of the potential prophylactic and therapeutic effects of Kaempferol on experimental *Trichinella spiralis* infection. *J. Helminthol.* **97**, e36 (2023).
37. Aderemi, A. V., Ayeleso, A. O., Oyedapo, O. O., Mukwevho, E. & Metabolomics A scoping review of its role as a tool for disease biomarker discovery in selected non-communicable diseases. *Metabolites* **11**, 418 (2021).
38. Yoon, D. W. et al. Untargeted metabolomics analysis of rat hippocampus subjected to sleep fragmentation. *Brain Res. Bull.* **153**, 74–83 (2019).
39. Denery, J. R., Nunes, A. A. K., Hixon, M. S., Dickerson, T. J. & Janda, K. D. Metabolomics-based discovery of diagnostic biomarkers for onchocerciasis. *PLoS Negl. Trop. Dis.* **4**(10), e834 (2010).
40. Liu, R. et al. Comparative metabolomics investigations of *Schistosoma Japonicum* from SCID mice and BALB/c mice: clues to developmental abnormality of schistosome in the immunodeficient host. *Front. Microbiol.* **10**, 440 (2019).
41. Uthailak, N. et al. Metabolite profiling of *Trichinella spiralis* adult worms and muscle larvae identifies their excretory and secretory products. *Front. Cell. Infect. Microbiol.* **13**, 1306567 (2023).
42. Zheng, W. et al. Serum metabolomic alterations in beagle dogs experimentally infected with *Toxocara canis*. *Parasit. Vectors.* **12**, 447 (2019).
43. Brenner, S. The genetics of caenorhabditis elegans. *Genetics* **77**, 71–94 (1974).
44. Smout, M. J., Kotze, A. C., McCarthy, J. S. & Loukas, A. A novel high throughput assay for anthelmintic drug screening and resistance diagnosis by real-time monitoring of parasite motility. *PLoS Negl. Trop. Dis.* **4**(11), e885 (2010).
45. Bischof, L. J., Huffman, D. L. & Aroian, R. V. Assays for toxicity studies in *C. elegans* with Bt crystal proteins. *Methods Mol. Biol.* **351**, 139–154 (2006).
46. Laohapaisan, P. et al. Discovery of N-methylbenzo[d]oxazol-2-amine as a new anthelmintic agent through a scalable protocol for the synthesis of N-alkylbenzo[d]oxazol-2-amine and N-alkylbenzo[d]thiazol-2-amine derivatives. *Bioorg. Chem.* **131**, 106287. https://doi.org/10.1016/j.bioorg.2022.106287 (2023).
47. Fongsodsri, K. et al. Sericin promotes chondrogenic proliferation and differentiation via Glycolysis and Smad2/3 TGF-beta signaling inductions and alleviates inflammation in three-dimensional models. *Sci. Rep.* **14**(1), 11553 (2024).
48. Kanaji, S., Iwahashi, J., Kida, Y., Sakaguchi, M. & Mihara, K. Characterization of the signal that directs Tom20 to the mitochondrial outer membrane. *J. Cell. Biol.* **151**(2), 277–288 (2000).
49. Lin, S. et al. Consolidating biallelic SDHD variants as a cause of mitochondrial complex II deficiency. *Eur. J. Hum. Genet.* **29**(10), 1570–1576 (2021).
50. Brooks, C. et al. Bak regulates mitochondrial morphology and pathology during apoptosis by interacting with Mitofusins. *Proc. Natl. Acad. Sci. U S A.* **104**(28), 11649–11654 (2007).
51. Chienwichai, P. et al. Untargeted serum metabolomics analysis of *Trichinella spiralis*-infected mouse. *PLoS Negl. Trop. Dis.* **17**(2), e0011119. https://doi.org/10.1371/journal.pntd.0011119 (2023).
52. Tsugawa, H. et al. MS-DIAL: data independent MS/MS Deconvolution for comprehensive metabolome analysis. *Nat. Methods.* **12**(6), 523–526 (2015).
53. Hahnel, S. R., Dilks, C. M., Heisler, I., Anderson, E. C. & Kulke, D. *Caenorhabditis elegans* in anthelmintic research – old model, new perspectives. *Int. J. Parasitol. Drugs Drug Resist.* **14**, 237–248 (2020).
54. Weaver, K. J., May, C. J. & Ellis, B. L. Using a health-rating system to evaluate the usefulness of *Caenorhabditis elegans* as a model for anthelmintic study. *PLoS ONE.* **12**(6), e0179376 (2017).
55. Boot, A. W., Haenen, G. R. M. M. & Bast, A. Health effects of quercetin: from antioxidant to nutraceutical. *Eur. J. Pharmacol.* **585**, 325–337 (2008).
56. Shi, M. D., Shiao, C. K., Lee, Y. C. & Shih, Y. W. Apigenin, a dietary flavonoid, inhibits proliferation of human bladder cancer T-24 cells via blocking cell cycle progression and inducing apoptosis. *Cancer cell. int.* **15**, 33 (2015).
57. Ayuda-Durán, B. et al. Exploring target genes involved in the effect of Quercetin on the response to oxidative stress in *Caenorhabditis elegans*. *Antioxidants* **8**, 585 (2019).
58. Ulusoy, H. G. & Sanlier, N. A minireview of quercetin: from its metabolism to possible mechanisms of its biological activities. *Crit. Rev. Food Sci. Nutr.* **60**(19), 3290–3303 (2020).
59. Akkari, H. et al. In vitro evidence that the pastoral Artemisia Campestris species exerts an anthelmintic effect on Haemonchus contortus from sheep. *Vet. Res. Commun.* **38**(3), 249–255 (2014).

60. Tang, F., Peng, W., Kou, X., Chen, Z. & Zhang, L. High-throughput screening identification of apigenin that reserves the colistin resistance of mcr-1-positive pathogens. *Microbiol. Spectr.* **12**(10), e0034124 (2024).
61. Chaniad, P., Mungthin, M., Payaka, A., Viriyavejakul, P. & Punsawad, C. Antimalarial properties and molecular Docking analysis of compounds from *Dioscorea Bulbufera* L. as new antimalarial agent candidates. *BMC Complement. Med. Ther.* **21**, 144 (2021).
62. Arzumanian, V. A., Kiseleva, O. I. & Poverennaya, E. V. The curious case of the HepG2 cell line: 40 years of expertise. *Int. J. Mol. Sci.* **22**, 13135 (2021).
63. Hiebl, V. et al. Caco-2 cells for measuring intestinal cholesterol transport-possibilities and limitations. *Biol. Proced. Online*. **22**, 7 (2020).
64. Choi, G. Y. et al. Acute drug-induced hepatitis caused by albendazole. *J. Korean Med. Sci.* **23**, 903–905 (2008).
65. Zuluaga, J. I. M., Castro, A. E. M., Cadavid, J. C. P. & Gutierrez, J. C. R. Albendazole-induced granulomatous hepatitis: a case report. *J. Med. Case Rep.* **7**, 201 (2013).
66. Oscanoa, T. J., Amado, J., Romero-Ortuno, R. & Carvajal, A. Hepatic disorders associated with the use of Ivermectin for SARS-CoV-2 infection in adults: a pharmacovigilance study in vigibase. *GHFBB* **15**(4), 426–429 (2022).
67. Veit, O., Beck, B., Steuerwald, M. & Hatz, C. First case of ivermectin-induced severe hepatitis. *Trans. R Soc. Trop. Med. Hyg.* **100**, 795–797 (2006).
68. Mendonça, J. C., Gama, L. A., Hauschildt, A. T., Corá, L. A. & Américo, M. F. Gastrointestinal effects of Ivermectin treatment in rats infected with *Strongyloides venezuelensis*. *Acta Trop.* **194**, 96–77 (2019).
69. Hussein, Y. A., Yahiya, Y. I. & Kadhim, S. F. Hepatoprotective, antioxidant, and anti-inflammatory properties of Quercetin in Paracetamol overdose-induced liver injury in rats. *Eurasian J. Med. Oncol.* **9**(2), 224–233 (2025).
70. Katsaros, I. et al. The effects of Quercetin on non-alcoholic fatty liver disease (NAFLD) and the role of Beclin1, P62, and LC3: an experimental study. *Nutrients* **16**, 4282 (2024).
71. Suzuki, T. & Hara, H. Quercetin enhances intestinal barrier function through the assembly of Zonula occludens-2, occludin, and claudin-1 and the expression of claudin-4 in Caco-2 cells. *J. Nutr.* **139**(5), 965–974 (2009).
72. Feng, J. et al. Quercetin alleviates intestinal inflammation and improves intestinal functions via modulating gut microbiota composition in LPS-challenged laying hens. *Poult. Sci.* **102**(3), 102433 (2022).
73. Liu, J. et al. Subchronic exposure of apigenin induces hepatic oxidative stress in male rats. *Health* **6**, 989–997 (2014).
74. Singh, P., Mishra, S. K., Noel, S., Sharma, S. & Rath, S. K. Acute exposure of apigenin induces hepatotoxicity in Swiss mice. *PLoS ONE* **7**(2), e31964 (2012).
75. Elmahy, R. A. & Radwan, N. A. *In vitro* evaluation of the nematicidal efficacy of Quercetin on adult *Toxocara canis*. *Acta Parasitol.* **70**, 96 (2025).
76. Tawari, S. G. et al. Metabolic adjustments of blood-stage *Plasmodium falciparum* in response to sublethal pyrazoleamide exposure. *Sci. Rep.* **12**, 1167 (2022).
77. Van der Kaaij, A., van Noort, K., Nibbering, P., Wilbers, R. H. P. & Schots, A. Glyco-engineering plants to produce helminth glycoproteins as prospective biopharmaceuticals: recent advances, challenges and future prospects. *Front. Plant. Sci.* **13**, 882835 (2022).
78. Milcheva, R. S., Petkova, S. L., Dubinský, P., Hurniková, Z. & Babál, P. Glycosylation changes in different development stages of *Trichinella*. *Biol* **64**, 180–186 (2009).
79. Bunte, M. J. M., Schots, A., Kammenga, J. E. & Wilbers, H. P. Helminth glycans at the host-parasite interface and their potential for developing novel therapeutics. *Front. Mol. Biosci.* **8**, 807821 (2022).
80. Márquez-Contreras, M. E. Mechanisms of immune evasion by *Trypanosoma brucei*. *Microbiol. Curr. Res.* **2**(3), 39–44 (2018).
81. Yeshi, K., Ruscher, R., Loukas, A. & Wangchuk, P. Immunomodulatory and biological properties of helminth-derived small molecules: potential applications in diagnostics and therapeutics. *Front. Parasitol.* **1**, 984152 (2022).
82. Chakraborty, A., Bayry, J. & Mukherjee, S. Helminth-derived biomolecules as potential therapeutics against ulcerative colitis. *Immunotherapy* **16**(10), 635–640 (2024).
83. Kim, I. S. & Jo, E. Inosine: a bioactive metabolite with mutimodal actions in human diseases. *Front. Pharmacol.* **13**, 1043970 (2022).
84. Zhang, Y., Morar, M. & Ealick, S. E. Structural biology of the purine biosynthetic pathway. *Cell. Mol. Life Sci.* **65**, 3699–3724 (2008).
85. Itsko, M. & Schaaper, R. M. dGTP starvation in *Escherichia coli* provides new insights into the thymineless-death phenomenon. *PLoS Genet.* **10**(5), e1004310 (2014).
86. Haim-Vilmovsky, L. et al. Mapping *Rora* expression in resting and activated CD4 + T cells. *PLoS ONE*. **16**(5), e0251233 (2021).
87. Hopwood, T. W. et al. The circadian regulator BMAL1 programmes responses to parasitic worm infection via a dendritic cell clock. *Sci. Rep.* **8**, 3782 (2018).
88. Rijo-Ferreira, F., Takahashi, J. S. & Figueiredo, L. M. Circadian rhythms in parasites. *PLoS Pathog.* **13**(10), e1006590 (2017).
89. Bougarne, N. et al. Molecular actions of PPARα in lipid metabolism and inflammation. *Endocr. Rev.* **39**(5), 760–802 (2018).
90. Chan, M. M., Evans, K. W., Moore, A. R. & Fong, D. Peroxisome proliferator-activated receptor (PPAR): Balance for survival in parasitic infections. *J. Biomed. Biotechnol.* **2010**, 828951 (2010).
91. Worgall, T. S. et al. Sterol and fatty acid regulatory pathways in a *Giardia lamblia*-derived promoter: evidence for SREBP as an ancient transcription factor. *J. Lipid Res.* **45**(5), 981–988 (2004).
92. He, T. et al. Lipid metabolism: the potential targets for toxoplasmosis treatment. *Parasit. Vectors*. **17**, 111 (2024).
93. Li, Y. L. et al. Biological characteristics of a new long-chain fatty acid transport protein 1 from *Trichinella spiralis* and its participation in lipid metabolism, larval moulting, and development. *Vet. Res.* **55**, 126 (2024).
94. Qi, W. et al. The ω-3 fatty acid α-linolenic acid extends *Caenorhabditis elegans* lifespan via NHR-49/PPARα and oxidation to Oxylipins. *Aging Cell.* **16**, 1125–1135 (2017).
95. Monteiro, J. P. et al. Evaluating fatty acid profiles in Anisakid nematode parasites and adjacent tissue of European Hake (*Merluccius merluccius*): a first insight into local host-parasite lipid dynamics. *Parasitol. Res.* **124**, 32 (2025).
96. Fahs, H. Z. et al. A new class of natural anthelmintics targeting lipid metabolism. *Nat. Commun.* **16**, 305 (2025).
97. Suliman, H. B. & Piantadosi, C. A. Mitochondrial biogenesis: regulation by endogenous gases during inflammation and organ stress. *Curr. Pharm. Des.* **20**(35), 5653–5662 (2014).
98. Sharma, S., Singha, U. K. & Chaudhuri, M. Role of Tob55 on mitochondrial protein biogenesis in *Trypanosoma brucei*. *Mol. Biochem. Parasitol.* **174**(2), 89–100 (2010).


## Acknowledgements

We are grateful to the member of the Department of Molecular Tropical Medicine and Genetics, Faculty of Tropical Medicine, Mahidol University for helpful discussions and advice in the development of our research.

## Author contributions

K.S. wrote the original draft, conducted review and editing, and performed investigation, validation, formal analysis, and data curation. N.N. contributed to review and editing and carried out investigation. P.A. provided resources, contributed methodology, and performed investigation. N.U. conducted investigation, formal analysis, and visualization. K.F. performed investigation, visualization, and formal analysis. T.K. carried out investi-

gation and visualization. S.A. provided resources and contributed methodology. T.T. contributed methodology and performed investigation. P.T. contributed methodology and investigation. J.T. contributed methodology and investigation. O.R. contributed to review and editing, supervised the work, provided resources, oversaw project administration, contributed methodology, secured funding, and conceptualized the study. All authors reviewed the manuscript.

## Funding

This research project is supported by Mahidol University (MU's Strategic Research Fund: 2023) to O.R. This research project was also supported by postdoctoral fellowships awarded by Mahidol University to N.N. and O.R.

## Declarations

## Competing interests

The authors declare no competing interests.

## Ethical approval

Animal experiments were approved by the Faculty of Tropical Medicine Animal Care and Use Committee (FTM-ACUC 032/2020), Mahidol University. All animal experiments were conducted in accordance with ARRIVE guidelines. All methods were performed in accordance with relevant guidelines and regulations.

## Additional information

**Supplementary Information** The online version contains supplementary material available at https://doi.org/10.1038/s41598-025-34049-5.

**Correspondence** and requests for materials should be addressed to O.R.

**Reprints and permissions information** is available at www.nature.com/reprints.

**Publisher's note** Springer Nature remains neutral with regard to jurisdictional claims in published maps and institutional affiliations.